New Equations for Electromagnetic Scattering by Small Perturbations of a Perfectly Conducting Surface

Dennis Holliday, Lester L. DeRaad, Jr., and Gaetan J. St-Cyr

***Abstract*—New equations are derived for the electromagnetic scattering produced by a small perturbation of a general perfectly conducting surface. These equations explicitly incorporate the magnetic field boundary condition on the general surface, which implies that the new Born term by itself leads to conventional backscatter formulas. The accuracy of the new equations is demonstrated by an example.**

***Index Terms*—Electromagnetic scattering, rough surfaces.**

I. Introduction

THE scattering of electromagnetic waves from rough surfaces is a basic phenomenon, which is important in a number of fields including, for example, radar ocean imaging. Rice [1] was the first to publish a useful theory of electromagnetic scattering from rough surfaces and his work has been a major influence on subsequent research. Using what is called the small perturbation method, Rice derived formulas that led to the average cross section per unit area for vertically and horizontally polarized backscatter from a perfectly conducting statistical rough surface

$$\sigma_{VV} = 8\pi\kappa^4(1+\sin^2\theta)^2[\psi(2\boldsymbol{\kappa}_H)+\psi(-2\boldsymbol{\kappa}_H)] \quad (1)$$

and

$$\sigma_{HH} = 8\pi\kappa^4(1-\sin^2\theta)^2[\psi(2\boldsymbol{\kappa}_H)+\psi(-2\boldsymbol{\kappa}_H)] \quad (2)$$

where κ is the magnitude of the incident wavenumber vector $-\boldsymbol{\kappa}$, which has $-\boldsymbol{\kappa}_H$ as its horizontal vector projection, θ is the incidence angle of the impinging electromagnetic wave relative to the vertical, and $\psi(\mathbf{k})$ is the wavenumber height spectrum of the rough surface, which is related to the surface-height correlation function by

$$\langle\eta(\mathbf{x}_1)\eta(\mathbf{x}_2)\rangle = \int d\mathbf{k}\psi(\mathbf{k})\cos\mathbf{k}\cdot(\mathbf{x}_1-\mathbf{x}_2) \quad (3)$$

$\eta(\mathbf{x})$ being the surface height at the horizontal position $\mathbf{x}$; the symbols $\langle\,\rangle$ denote an average over the statistical ensemble that describes the rough surface.

Equations (1) and (2), which have a number of remarkable implications, are derived under the conditions that $|\nabla\eta| \ll 1$ and $\kappa|\eta| \ll 1$, which are too restrictive for many scatterers of interest, such as ocean waves, where $|\nabla\eta|$ can be greater than 1 and $\kappa|\eta| \gg 1$. For these latter conditions, it is conventional to invoke the "composite approximation" in which small amplitude resonant waves, to which (1) and (2) apply, ride on long wavelength waves of large amplitude—and possibly large slope—that are assumed to be *flat locally* so that (1) and (2) can be applied with θ being an equivalent incidence angle measured relative to the normal of the long wavelength surface [2].

The composite approximation has not led to a successful model of low grazing angle ocean backscatter at high radar frequencies, such as X-band (10 GHz). For example, (1) and (2) predict, even after corrections are made for imperfectly conducting sea water, that

$$\sigma_{VV} \gg \sigma_{HH} \quad (4)$$

at low grazing angles ($\theta \geq 80^\circ$) with differences typically greater than 20 dB. However, there are many ocean backscatter data where σ_{VV} and σ_{HH} are within a few decibels of each other [3]. In addition, a significant component of low grazing angle ocean backscatter is composed of sea spikes for which σ_{HH} has been observed to be much larger than σ_{VV} [4]. These discrepancies suggest that the applicability of the composite approximation to ocean-like waves be questioned, which has led us to a new set of equations for scattering from perfectly conducting surfaces.

Specifically, for a given incident electromagnetic wave, we consider the changes in surface current produced by the addition of a small perturbation $\eta_R(\mathbf{x})$ to a *general* perfectly conducting surface $z = \eta_L(\mathbf{x})$. The surface $\eta_L(\mathbf{x})$ may have regions where $\kappa|\eta_L| \gg 1$ as well as large values of $|\nabla\eta_L|$. The surface $\eta_L(\mathbf{x})$ can also, if one wishes, be restricted to have only low wavenumber components so that resonant backscatter from such a surface will be small. For such a case, the perturbation $\eta_R(\mathbf{x})$ can also be chosen to have large wavenumber components so that it alone is responsible for backscatter. Our results can also be extended to random surfaces or to random perturbations of nonstochastic surfaces.

We begin in Section II with a review of the equations that comprise the conventional surface current integral equation (SCIE) theory of scattering from a perfectly conducting surface. This theory will then be reformulated in Section III to derive a new integral equation for a linear current $\mathbf{j}_R(\mathbf{x})$ that results when $\eta_R(\mathbf{x})$ is added to $\eta_L(\mathbf{x})$. This equation will be seen to differ significantly from the composite approximation.

Manuscript received September 25, 1995; revised June 30, 1998. This work was supported by the Office of Under Secretary of Defense, Intelligence System Support Organization (ISSO), Ms. Donna Kulla, Program Manager, under Contract DMA800-94-C-6010.

The authors are with Logicon RDA, Los Angeles, CA 90009 USA.

Publisher Item Identifier S 0018-926X(98)07489-4.

Formulas for the scattered field and the Rice limit, which results in (1) and (2), will be shown in Section IV to be obtained from the formulas of Section III. In Section V, we use the new equations to predict backscatter from the "exponential" wedge, a problem that has been solved accurately by a previous method [5]. A summary of conclusions is presented in Section VI.

II. Review and Definitions

The magnetic induction $\mathbf{B}(F)e^{-i\omega t}$ produced by the scattering of an incoming field $\mathbf{B}_{in}(F)e^{-i\omega t}$ at a point $\mathbf{r}_F = \mathbf{x}_F + \hat{e}_z z_F$ above a perfectly conducting surface $z_1 = \eta(\mathbf{x}_1) \equiv \eta(1)$, where $\mathbf{x}_F$ is the horizontal vector component of the point F, is given by the Stratton–Chu equation

$$\mathbf{B}(F) = \mathbf{B}_{in}(F) - \int_S d\mathbf{x}_1 [\mathbf{n}(1) \times \mathbf{B}(1)] \times \nabla^{(1)} G(F, 1) \quad (5)$$

S denotes the surface $\eta(1)$, which is assumed to be a Lyapunov surface, $\nabla^{(1)}$ indicates a gradient taken with respect to the position vector $\mathbf{r}_1$,

$$G(F, 1) = -\frac{1}{4\pi} \frac{1}{|\mathbf{r}_F - \mathbf{r}_1|} \exp[i\kappa |\mathbf{r}_F - \mathbf{r}_1|] \quad (6)$$

$$\mathbf{n}(1) = -\nabla \eta(\mathbf{x}_1) + \hat{e}_z \quad (7)$$

where $\hat{e}_z$ is the vertical unit vector, $\mathbf{x}_1$ is the horizontal vector projection of $\mathbf{r}_1$, and

$$\kappa = \omega / c \quad (8)$$

c is the speed of light. Stratton [6, sections 8.14 and 8.15], presents a straightforward derivation of (5) from Maxwell's equations. The reader should note that $\mathbf{n} \times \mathbf{E}$ and $\mathbf{n} \cdot \mathbf{B}$ are both zero on the perfectly conducting surface; $\mathbf{E}$ is the electric field.

When the point F is taken to approach $z = \eta(\mathbf{x})$ in (5), the surface current integral equation is obtained

$$\mathbf{j}(1) = \mathbf{j}_{in}(1) - 2\mathbf{n}(1) \times \int_S d\mathbf{x}_2 \mathbf{j}(2) \times \nabla^{(2)} G(1, 2) \quad (9)$$

where

$$\mathbf{j}(1) = \mathbf{n}(1) \times \mathbf{B}(1) \quad (10)$$

and

$$\mathbf{j}_{in}(1) = 2\mathbf{n}(1) \times \mathbf{B}_{in}(1) \quad (11)$$

it is to be noted that both points 1 and 2 are on the surface $z = \eta(\mathbf{x})$. An important property of the solution of (9) is that $\mathbf{j}(1)$ is *on* the surface:

$$\mathbf{n}(1) \cdot \mathbf{j}(1) = 0. \quad (12)$$

In the derivation of (9) from (5) it is implicit that

$$\mathbf{n}(1) \cdot \mathbf{B}_{in}(1) = \mathbf{n}(1) \cdot \int_S d\mathbf{x}_2 \mathbf{j}(2) \times \nabla^{(2)} G(1, 2) \quad (13)$$

which is a consequence of $\mathbf{n} \cdot \mathbf{B} = 0$ on S.

When the point F is many wavelengths away from the scattering region, (5) can be used to write the scattered field as

$$\mathbf{B}_S(F) = \mathbf{B}(F) - \mathbf{B}_{in}(F) \Rightarrow -\frac{i}{4\pi} \frac{\exp(i\kappa r_F)}{r_F} \int_S d\mathbf{x}_1 \mathbf{j}(1) \times \mathbf{k} \cdot \exp[-i\mathbf{k}_H \cdot \mathbf{x}_1 - ik_z \eta(1)] \quad (14)$$

where $r_F = |\mathbf{x}_F + \hat{e}_z z_F|$

$$\mathbf{k} = \frac{\mathbf{r}_F}{r_F} \kappa \quad (15)$$

and the incoming field in (5) has the form

$$\mathbf{B}_{in}(F) = \mathbf{B}_0 \exp[-i\boldsymbol{\kappa}_H \cdot \mathbf{x}_F - i\kappa_z z_F]. \quad (16)$$

III. New Equations

In this section, we will derive equations that can be used to compute that part of the scattered field $\mathbf{B}_S$ that is linear in the amplitude of the perturbation η_R when an expansion of the basic scattering equation is made. The implicit assumption behind this procedure is that these expansions do converge so that the resulting linear equations are useful for sufficiently small values of $\kappa\eta_R$ and $|\nabla\eta_R|$, an issue that will be investigated numerically.

To begin we define

$$\mathbf{j}(A) = \mathbf{j}_L(A) + \mathbf{j}_R(A) + \mathbf{j}_E(A) \quad (17)$$

where $\mathbf{j}_L$ is the current induced on $z = \eta_L$ when $\eta_R = 0$, $\mathbf{j}_R$ is a linear functional of η_R and $\mathbf{j}_E$ is higher order in η_R. Substituting (17) in both sides of (9) and separating out terms linear in η_R, we obtain

$$\mathbf{j}_R(1) = \mathbf{j}_R^{(in)}(1) - 2\mathbf{n}_L(1) \times \int_L d\mathbf{x}_2 \mathbf{j}_R(2) \times \mathbf{R}_L(1, 2) Q_L(1, 2) \quad (18)$$

where

$$\mathbf{j}_R^{(in)}(1) = -\nabla\eta_R(1) \times \left\{ 2\mathbf{B}_0 \exp[-i\boldsymbol{\kappa}_H \cdot \mathbf{x}_1 - i\kappa_z \eta_L(1)] - 2\int_L d\mathbf{x}_2 \mathbf{j}_L(2) \times \mathbf{R}_L(1, 2) Q_L(1, 2) \right\} + \boldsymbol{\Lambda}_R(1) \quad (19)$$

with

$$\boldsymbol{\Lambda}_R(1) = -i\kappa_z \eta_R(1) \mathbf{j}_L^{(in)}(1) - 2\mathbf{n}_L(1) \times \int_L d\mathbf{x}_2 \mathbf{j}_L(2) \cdot \left\{ \hat{e}_z [\eta_R(1) - \eta_R(2)] Q_L(1, 2) + \mathbf{R}_L(1, 2) \frac{1}{4\pi} \frac{\exp[i\kappa R_L(1, 2)]}{R_L(1, 2)^3} \cdot [-\kappa^2 R_L(1, 2)^2 - 3i\kappa R_L(1, 2) + 3] \cdot \frac{\eta_L(1) - \eta_L(2)}{R_L(1, 2)} \cdot \frac{\eta_R(1) - \eta_R(2)}{R_L(1, 2)} \right\} \quad (20)$$

$\mathbf{j}_L$ satisfies (9) on the surface $z = \eta_L(\mathbf{x})$

$$\mathbf{j}_L^{(in)}(1) = 2\mathbf{n}_L(1) \times \mathbf{B}_0 \exp[-i\boldsymbol{\kappa}_H \cdot \mathbf{x}_1 - i\kappa_z \eta_L(1)] \quad (21)$$

$$\mathbf{n}_L(1) = -\nabla\eta_L(1) + \hat{e}_z \quad (22)$$

$$\mathbf{R}_L(1,2) = \mathbf{x}_1 - \mathbf{x}_2 + \hat{e}_z[\eta_L(1) - \eta_L(2)] \tag{23}$$

$$Q_L(1,2) = \frac{1}{4\pi}\frac{\exp[i\kappa R_L(1,2)]}{R_L(1,2)^3}[i\kappa R_L(1,2) - 1]. \tag{24}$$

A significant simplification of the above equations is possible. From (12) we obtain the condition

$$\mathbf{n}_L(1)\cdot\mathbf{j}_R(1) = \nabla\eta_R(1)\cdot\mathbf{j}_L(1) \tag{25}$$

so that only the tangential component (with respect to the surface η_L) of $\mathbf{j}_R$ is determined by (18). Next we see that (13) implies that the component of the $\{\}$ in the first term in (19) in the $\mathbf{n}_L$ direction is zero. These conditions result in

$$\mathbf{j}_R^{(T)}(1) = \mathbf{j}_R^{(0)}(1) - 2\mathbf{n}_L(1)\times\int_L d\mathbf{x}_2\mathbf{j}_R^{(T)}(2) \times \mathbf{R}_L(1,2)Q_L(1,2) \tag{26}$$

where

$$\mathbf{j}_R^{(0)}(1) = -\mathbf{j}_L(1)\frac{\mathbf{n}_L(1)\cdot\nabla\eta_R(1)}{|\mathbf{n}_L(1)|^2} - 2\mathbf{n}_L(1) \times\int_L d\mathbf{x}_2\mathbf{n}_L(2)\times\mathbf{R}_L(1,2) \cdot Q_L(1,2)\frac{\nabla\eta_R(2)\cdot\mathbf{j}_L(2)}{|n_L(2)|^2} + \boldsymbol{\Lambda}_R(1) \tag{27}$$

and

$$\mathbf{j}_R^{(T)}(1) = -\frac{\mathbf{n}_L(1)\times[\mathbf{n}_L(1)\times\mathbf{j}_R(1)]}{|\mathbf{n}_L(1)|^2} \tag{28}$$

so that

$$\mathbf{j}_R(1) = \mathbf{j}_R^{(T)}(1) + \mathbf{n}_L(1)\frac{\nabla\eta_R(1)\cdot\mathbf{j}_L(1)}{|\mathbf{n}_L(1)|^2}. \tag{29}$$

Equations (20) and (26)–(29) comprise the new equations for the perturbed current $\mathbf{j}_R$. When the surface $z = \eta_L(y)$ is flat and $\mathbf{j}_L$ is $2\mathbf{n}\times\mathbf{B}_{\text{incident}}$, the above equations reduce to the conventional composite model.

Equations (26)–(29) were obtained by perturbing the surface current integral equation. To produce these results it was useful to write the integral equation with reference to coordinates that do not change when the surface is perturbed. The procedure for solving for $\mathbf{j}_R$ is first to obtain $\mathbf{j}_L$ from (9) on $z = \eta_L(\underline{x})$, then determine $\mathbf{j}_R^{(0)}$ from (27), and, finally, to solve (26) for $\mathbf{j}_R^{(T)}$, which is used in (29) to find $\mathbf{j}_R$.

The derivation of (26) and (27) can be viewed as an extension of Rice's earlier work [1]. Where Rice used a differential formulation of the scattering problem to consider perturbations from a plane, we use an integral formulation because it is a more convenient description of the scattering problem for a general surface $z = \eta_L$.

IV. Perturbed Scattered Field and Rice Limit

From (14) and the relationship $\mathbf{E}_S = -\hat{k}\times\mathbf{B}_S$, we obtain an expression for the perturbed scattered electric field in a polarization direction $\hat{e}(\mathbf{k})$

$$\hat{e}(\mathbf{k})\cdot\mathbf{E}_S(F) = \frac{ik}{4\pi}\frac{\exp[i\kappa r_F]}{r_F}\int_S d\mathbf{x}_1\hat{e}(\mathbf{k}) \cdot\{-ik_z\eta_R(1)\mathbf{j}_L(1) + \mathbf{j}_R(1)\} \cdot\exp[-i\mathbf{k}_H\cdot\mathbf{x}_1 - ik_z\eta_L(1)] \tag{30}$$

where $\hat{e}(\mathbf{k})$ is some linear combination of the two orthonormal polarization vectors of the scattered field

$$\hat{e}_H(\mathbf{k}) = \hat{k}_H\times\hat{e}_z \tag{31}$$

$$\hat{e}_V(\mathbf{k}) = \hat{e}_H(\mathbf{k})\times\hat{k} = -\frac{k_z}{\kappa}\hat{k}_H + \frac{k_H}{\kappa}\hat{e}_z. \tag{32}$$

Once $\mathbf{j}_L$ and $\mathbf{j}_R$ are determined from their integral equations, (30) can be used to compute the components of the scattered electric field.

For backscatter, where $\mathbf{k} = \boldsymbol{\kappa}$, (30) leads to (1) and (2) for $\eta_L = 0$ as will now be shown. Since $\mathbf{n}_L = \hat{e}_z$, we obtain

$$\mathbf{j}_L(1) = 2\hat{e}_z\times\mathbf{B}_0\exp[-i\boldsymbol{\kappa}_H\cdot\mathbf{x}_1] \tag{33}$$

which produces no backscatter and

$$\mathbf{j}_R(1) = -i\kappa_z\eta_R(1)\mathbf{j}_L(1) + \nabla\eta_R(1)\cdot\mathbf{j}_L(1)\hat{e}_z - 2\hat{e}_z \times\int d\mathbf{x}_2 Q_L(1,2)\{\mathbf{j}_L(2)\times\hat{e}_z[\eta_R(1) - \eta_R(2)] + \hat{e}_z\times(\mathbf{x}_1 - \mathbf{x}_2)\nabla\eta_R(2)\cdot\mathbf{j}_L(2)\} \tag{34}$$

from (9) and (26)–(29), respectively. Substituting (33) and (34) into (30), we get for backscatter

$$\hat{e}(\boldsymbol{\kappa})\cdot\mathbf{E}_S(F) = \frac{1}{4\pi}\frac{\exp[i\kappa r_F]}{r_F}\hat{e}(\boldsymbol{\kappa})\cdot[\mathbf{E}_0\kappa_z^2 + 2\hat{e}_z\hat{e}_z\cdot\mathbf{E}_0\kappa^2] \cdot\int d\mathbf{x}_1\eta_R(1)\exp(-i2\boldsymbol{\kappa}_H\cdot\mathbf{x}_1) \tag{35}$$

where the result

$$\int d\mathbf{x}\mathbf{x}\frac{1}{4\pi}\frac{\exp(i\kappa|\mathbf{x}|)}{|\mathbf{x}|^3}(i\kappa|\mathbf{x}| - 1)\exp(-i\mathbf{k}_H\cdot\mathbf{x}) = -\frac{1}{2}\frac{\mathbf{k}_H}{\sqrt{\kappa^2 - k_H^2}} \tag{36}$$

has been used and the incident electric field amplitude vector is obtained from $\mathbf{B}_0 = -\hat{\kappa}\times\mathbf{E}_0$.

When η_R is a random process with a wavenumber spectrum defined by (3), the cross section per-unit-area is defined as

$$\sigma = \lim_{r_F\to\infty}\frac{1}{\text{AREA}}\frac{4\pi r_F^2}{|\mathbf{E}_0|^2}\langle|\hat{e}(\boldsymbol{\kappa})\cdot\mathbf{E}_S|^2\rangle \tag{37}$$

where $\langle\,\rangle$ denotes the stochastic average and AREA is the area of the surface illuminated by the incident wave. Using (31) and (32) to define the polarization vector in (35), substituting the result in (37), and employing (3), we obtain (1) and (2).QED

Note, in contrast to the derivation in Holliday [7], this demonstration requires no overt iteration to show that the Rice resonant backscatter formulas are obtained. By incorporating the implications of the perfectly conducting boundary condition, i.e., (13), we have derived a new integral equation for the perturbed current $\mathbf{j}_R$ that manifests in its inhomogeneous term the difference between the amplitudes of VV and HH backscatter. This difference, which is very large at low grazing angles, is thus seen to be an important consequence of the boundary conditions.

V. The Exponential Wedge

Previously [5], we calculated the backscatter from a series of filtered exponential wedges by the method of forward–backward. We will here repeat these calculations using the new set of equations (9) for $\mathbf{j}_L$ [see (21)–(24)], and (26) for $\mathbf{j}_R^{(T)}$. These calculations will be for azimuthally homogeneous surfaces so that the cross track (here x) integral is performed in these equations. The unfiltered surface is given by [5]

$$\begin{aligned}\eta(y) &= \frac{A}{2}\left(1+\cos\frac{\pi y}{L}\right)\exp(-s|y|/A), \quad |y|\le L \\ &= 0 \qquad\qquad\qquad\qquad\qquad\quad |y| > L,\end{aligned} \tag{38}$$

which has a Fourier transform of $\tilde{\eta}(k)$. We now define two filters

$$F_L(k) = \begin{cases} 1, & |k| < 150 \\ \dfrac{1}{2}\left(1+\cos\pi\dfrac{|k|-150}{150}\right), & 150 \le |k| \le 300 \\ 0, & |k| > 300 \end{cases} \tag{39}$$

and

$$F(k) = \begin{cases} 1, & |k| < 1200 \\ \dfrac{1}{2}\left(1+\cos\pi\dfrac{|k|-1200}{1200}\right), & 1200 \le |k| \le 2400 \\ 0, & |k| > 2400. \end{cases} \tag{40}$$

The filter $F(k)$ was used in [5] to define the surface. We now define the long-wave surface $\eta_L(y)$ as the low wavenumber part of $\eta(y)$, namely,

$$\eta_L(y) = \frac{1}{2\pi}\int_{-\infty}^{+\infty}\tilde{\eta}(k)F_L(k)e^{iky}\,dk \tag{41}$$

and the perturbation $\eta_R(y)$, which is the high wavenumber part of $\eta(y)$ as

$$\eta_R(y) = \frac{1}{2\pi}\int_{-\infty}^{+\infty}\tilde{\eta}(k)[F(k)-F_L(k)]e^{iky}\,dk. \tag{42}$$

The sum of these surfaces is exactly the surface employed in [5], where $L = 1$ m and $s = \tan 22°$. For the parameters chosen, $\eta_R(y)$ is essentially independent of A, except for very small A. Fig. 1 shows $\eta_R(y)$ for $A = 1, 2, 4, 6, 8, 10$, and 12 cm; it has the form of a localized wave packet with a peak amplitude of about 1 mm. For $A = 0.1$ cm, η_R has a similar shape with a peak amplitude of about 1/2 mm. Since $\eta_R(y)$ is small compared with $\eta_L(y)$, it is reasonable to treat it as a perturbation.

We have solved (9) and (26) by two different methods and have compared the computed backscatter from (30) with that calculated by the forward–backward method for the full surface η, which has been shown to be accurate [5]. The two methods are:

1) solve (9) for $\mathbf{j}_L$ on η_L by forward–backward to an accuracy of 10^{-3} and solve (26) for $\mathbf{j}_R^{(T)}$ by forward–backward to an accuracy of 10^{-6};
2) solve (9) by *one* forward pass and solve (26) by *one* backward pass.

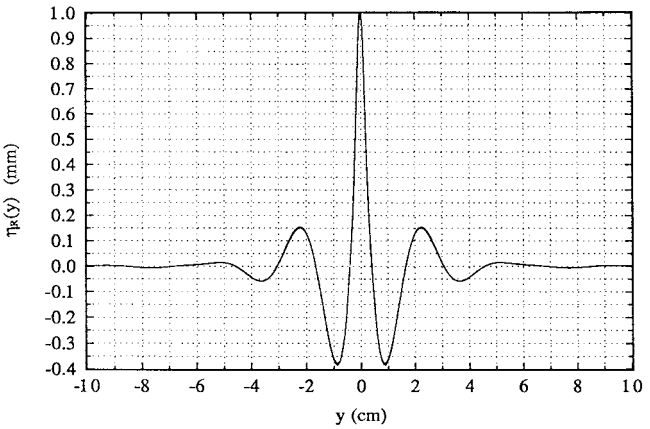

Fig. 1. η_R for $A = 1, 2, 4, 6, 8, 10, 12$ cm.

TABLE I
V-pol Backscatter Results

A (cm)	Forward-Backward Amplitude	Forward-Backward Phase (deg)	(1) dB	(1) deg	(2) dB	(2) deg
0.1	9.10×10^{-1}	−91.3	−0.5	−0.2	−0.5	−0.2
1	2.62	−120.0	−0.5	0.1	−0.5	1.2
2	3.35	−129.4	−0.5	0.0	−0.5	1.3
4	3.84	−133.9	−0.5	−0.1	−0.5	1.2
6	2.97	−128.0	−0.5	−0.5	−0.5	0.7
8	1.33	−106.7	−0.5	−1.1	−0.5	0.1
10	2.28×10^{-1}	0.5	−0.8	−1.3	−0.8	−0.5
12	1.10	177.8	−0.7	1.0	−0.7	2.3

TABLE II
H-pol Backscatter Results

A (cm)	Forward-Backward Amplitude	Forward-Backward Phase (deg)	(1) dB	(1) deg	(2) dB	(2) deg
0.1	3.74×10^{-3}	−94.2	−0.9	1.0	−0.9	0.8
1	1.91×10^{-2}	−166.3	−0.9	5.9	−0.6	4.0
2	3.67×10^{-2}	159.4	−0.8	5.3	−0.6	3.3
4	8.52×10^{-2}	120.6	−0.8	3.7	−0.7	0.8
6	1.44×10^{-1}	96.4	−0.8	2.6	−0.6	−1.1
8	1.95×10^{-1}	79.5	−0.8	1.6	−0.5	−2.5
10	2.15×10^{-1}	67.0	−0.8	0.8	−0.5	−3.3
12	1.87×10^{-1}	56.1	−1.0	1.1	−0.5	−3.0

As in [5] all calculations are performed at X-band (3-cm wavelength) at an incidence angle of 85°. Table I summarizes the backscatter results for incident V pol and Table II summarizes the results for incident H pol. Each table presents an accurate value of the magnitude and phase of the backscatter computed using forward–backward and a comparison between these results and the results computed by methods 1) and 2). The comparison is made between the amplitude squared values

(in decibels) and the phases (in degrees). For example, Table I shows for V-pol incident with $A = 10$ cm that method 1) produces a backscatter (amplitude)^2 value 0.8 dB below that obtained from the full forward–backward method and a backscatter phase 1.3° smaller.

One can see that both methods 1) and 2) result in accurate values, especially in V pol. The results of method 1) show that the new perturbation equations can be highly accurate and the results of method 2) shows that a less accurate method of solving the new equations, a single forward pass for $\mathbf{j}_L$ and a single backward pass for $\mathbf{j}_R^{(T)}$, produces acceptable values.

The comparison between the forward–backward results for the full surface η and the results from (9) and (26) shows that η_R is almost completely responsible for the backscatter because $\mathbf{j}_L$ does not appear in (30) as a source of backscatter. Since η_R is localized at the apex of the exponential wedge, as shown in Fig. 1, the backscatter from the exponential wedge will, when it is resolved in range, be seen to be produced near the apex. Consequently, a simple view of backscatter from the exponential wedge is that the change in slope at the apex of the wedge produces an η_R with spectral components that cause significant backscatter.

One might ask if a "composite approximation" could be used to calculate backscatter from the exponential wedge. Since the extent of η_R, according to Fig. 1, encompasses a wide range of slopes from $\nabla\eta_L \cong -0.4$ to $\nabla\eta_L \cong 0.4$, it is apparent that η_R does not "ride" on a flat surface so the heuristic rationale behind the "composite approximation"—that the surface underlying η_R is flat—is not applicable.

The σ_{HH}/σ_{VV} ratio for backscatter from the exponential wedge at 85° incidence angle can be seen to vary considerably with the amplitude of the wedge. At $A = 0.1$ cm, Tables I and II show that the ratio is -47.7 dB rising to a peak of -0.5 dB at $A = 10$ cm before falling to a value of -15.4 dB at $A = 12$ cm.

As mentioned above, the localized wave packet $\eta_R(y)$ is essentially identical for $A \geq 1$ cm (see Fig. 1) even though the variation in backscatter cross section over the domain $A = 1$ cm to $A = 12$ cm is 24 dB in V pol and 21 dB in H pol. These variations cannot, therefore, be due to changes in the resonant component of $\eta_R(y)$. Instead, our results demonstrate the unusual sensitivity of $\mathbf{j}_R$ to the long wave current $\mathbf{j}_L$. The importance of $\mathbf{j}_L$ can be seen from the integral equation for $\mathbf{j}_R^{(T)}$ (26) where a central quantity is the product $\eta_R(y)\mathbf{j}_L(y)$. To date, we have not identified the essential features of $\mathbf{j}_L$ that produce the large variations in backscatter. Multiple scattering is clearly responsible, but the effect is more complicated than simple interference between a direct ray and a reflected ray.

VI. Summary and Conclusions

We have derived new equations (26)–(29) that describe the electromagnetic scattering produced by a small perturbation of a general perfectly conducting surface. Because it incorporates the boundary condition $\mathbf{n} \cdot \mathbf{B} = 0$ on the unperturbed surface, the inhomogeneous or Born term of the new equations manifests the difference between the amplitudes of VV and HH backscatter in contrast to the usual Born term, which is independent of polarization. This new Born term by itself is responsible for the resonant backscatter results, (1) and (2), usually obtained by the small perturbation method [1] or by an iteration of the surface current integral equations [7].

A solution of the new equations was shown to produce accurate results for a test surface, the exponential wedge for which there is no unambiguous way to apply the "composite approximation" as it is conventionally understood. The backscatter from an exponential wedge with an amplitude of several electromagnetic wavelengths was shown to be produced by spectral components that result primarily from the change in slope at the apex of the wedge. Since these spectral components are localized at the apex of the wedge, the region responsible for the backscatter will be similarly localized.

References

[1] S. O. Rice, "Reflection of electromagnetic waves from slightly rough surfaces," *Commun. Pure Appl. Math.*, vol. 4, pp. 351–378, 1951.

[2] J. W. Wright, "A new model for sea clutter," *IEEE Trans. Antennas Propagat.*, vol. AP-16, pp. 217–223, Mar. 1968.

[3] M. W. Long, "On the polarization and the wavelength dependence of sea echo," *IEEE Trans. Antennas Propagat.*, vol. AP-13, pp. 749–754, Sept. 1965.

[4] D. B. Trizna, J. P. Hansen, P. Hwang, and J. Wu, "Laboratory studies of radar sea spikes at low grazing angles," *J. Geo. Res.*, vol. 96, pp. 12 529–12 537, July 1991.

[5] D. Holliday, L. L. DeRaad, Jr., and G. J. St-Cyr, "Forward–backward: A new method for computing low-grazing angle scattering," RDA-TR-2190001-002, Logicon R&D Assoc., Los Angeles, CA, Apr. 1995; *IEEE Trans. Antennas Propagat.*, vol. 44, May 1996.

[6] J. A. Stratton, *Electromagnetic Theory.* New York, NY: McGraw-Hill, 1941.

[7] D. Holliday, "Resolution of a controversy surrounding the Kirchoff approach and the small perturbation method in rough surface scattering theory," *IEEE Trans. Antennas Propagat.*, vol. AP-35, pp. 120–122, Jan. 1987.

Dennis Holliday received the B.S. degree in engineering science from Stanford University, Stanford, CA, in 1957, and the Ph.D. degree in theoretical physics from Princeton University, Princeton, NJ, in 1961.

From 1963 to 1971, he was a Member of the Physics Department of the Rand Corporation, Santa Monica, CA, where he worked on scattering theory, quantum optics, and quantum electronics, quantum statistical mechanics, nuclear proliferation technology, economics and policy, economics of nuclear power, and retirement plan formulation. He is currently with Logicon R&D Associates, Los Angeles, CA, where he conducts research for the Remote Imaging Program for the Office of the Under Secretary of Defense. He has published numerous reports and scientific papers. His research interests include radar scattering theory, the generation and interaction of internal waves in the ocean, and remote sensing of the sea surface.

Dr. Holliday is a member of the Working Group on Nuclear Proliferation and Arms Control of the California Arms Control and Foreign Policy Seminar, Phi Beta Kappa, Sigma Xi, and Tau Beta Pi. In 1960 and 1961, he was a NATO Postdoctoral Fellow in theoretical physics.

Lester L. DeRaad, Jr. received the B.S. degree in physics from the University of Minnesota, Minneapolis, in 1963, and the M.S. and Ph.D. degrees in physics from Harvard University, Cambridge, MA, in 1964 and 1970, respectively.

He served for several years as an Adjunct Assistant Professor at the University of California, Los Angeles, researching elementary particle physics, in particular, source theory, quantum electrodynamics, and strong and weak interaction phenomenology. He joined Logicon R&D Associates, Los Angeles, CA, in 1978, where he participated in the SXTF/BACCARAT project for DNA, developing simple plasma models for colliding wires and accelerating foils in pulse-power devices, and analyzing experimental data. He has conducted research in electromagnetic scattering, synthetic aperture radar, hydrodynamics, nuclear effects on communication systems, nuclear effects on radar systems, electromagnetic pulse, solid-state physics, and plasma science. In 1987, he joined the Radar Ocean Imaging project for the Office of the Under Secretary of Defense at Logicon, investigating electromagnetic scattering from random surfaces, studying hydrodynamic models of surface features of interest, and analyzing and interpreting experimental data.

Gaetan J. St-Cyr received the B.S., M.S., and Ph.D. degrees in electrical engineering from the California Institute of Technology, Pasadena, CA, in 1962, 1963, and 1969, respectively.

In 1962, he joined the Hughes Aircraft Company, where he participated in researching optimization techniques for infrared scanning systems, atmospheric radiance and transmissivity, light scattering by atmospheric aerosols and clouds, infrared background clutter, and missile countermeasure techniques. In 1971 he joined Cerberonics, where he directed research in weapons systems analysis and the design of missile countermeasure devices. In 1975 he participated in the foundation of Poseidon Research, where he managed programs on the recovery of sonar pulses buried in noise and on the detection of target signatures in random background noise. He created the Poseidon Hydro Code and numerical techniques to study fluid flow for hydrodynamic applications. In 1982 he joined Logicon R&D Associates, Los Angeles, CA, as a Research Scientist. He is currently working for the Office of the Under Secretary of Defense. His most recent research has been in the modeling of radar ocean imaging, signal detection, and data analysis.